3 Measurement of the Neutrino Magnetic Moment at the Bugey Nuclear Reactor

C. Amsler, P. Giarritta, M. Heinzelmann, O. Link, and F. Ould-Saada

In collaboration with Universität Bochum, Institut des Sciences Nucléaires (Grenoble), Université de Neuchâtel, Università di Padova
(MUNU Collaboration)

The MUNU experiment studies low energy $\overline{\nu}_e e^-$ elastic scattering at the Bugey nuclear power plant (2.8 GW thermal power) near Lyon. Its aim is to improve on the present laboratory upper limit for the magnetic moment of the electron neutrino ($1.8 \times 10^{-10} \mu_B$) by an order of magnitude. A magnetic moment of the order of a few 10^{-11} μ_B would lead to spin precession in the solar magnetic field [1] and could explain the deficit of solar neutrinos.

The motivations to perform such an experiment are as follows:

- Models of stellar evolution or the neutrino pulse from supernova SN 1987A set upper limits which are an order of magnitude smaller than can be achieved by our laboratory experiment. However, one should stress that the upper limit from SN 1987A ($< 10^{-12} \mu_B$) applies to Dirac and not to Majorana neutrinos.
- The earlier Savannah plant data [2] - together with today's knowledge of ^{235}U reactor spectra - point to a finite magnetic moment in the range $(2-4) \times 10^{-10} \mu_B$ [3].
- By measuring for the first time the angular distribution of $\overline{\nu}_e e^-$ scattering around 1 MeV neutrino energy we will determine the Weinberg angle with a precision of 5%, comparable to that achieved in high energy $\nu_\mu e^-$ scattering.

In contrast to previous experiments, we measure both the angle and the energy of the recoil electron. In the laboratory the electron is emitted into the forward hemisphere but the magnetic moment contribution increases with increasing recoil angle (and therefore with decreasing electron energy). Hence a low energy threshold for detecting the electron is essential. Our proposal assumed a threshold of 500 keV, determined by background. The background (isotropic and expected to be 4 events/day) can be measured with reactor on by looking at events with electrons emitted into the backward hemisphere - this is where the measurement of the recoil angle is particularly useful. Another advantage of measuring both the angle and the energy of the electron is the capability to reconstruct the incident neutrino energy.

The expected signal rate is 10 events/day if $\mu_\nu = 0$ and 13 events/day if $\mu_\nu = 10^{-10}\mu_B$. If background permits, we will lower the electron threshold and reduce the pressure to increase the track lengths. For example, with a threshold of 100 keV the signal rate would increase to 40, respectively 20 events/day. This would allow a measurement of the magnetic moment at the level of $10^{-11}\mu_B$ in one year of data taking.

The detector is located in the basement below reactor Nr. 5 at a distance of 18.6 m from the core, where the flux of cosmic ray muons is attenuated by 20 m of water equivalent. The intensity of antineutrinos reaching the detector is 10^{13} s^{-1} cm^{-2}. The detector consists of a time projection chamber (TPC) filled with CF_4 gas at 5 bar, 158 cm long and 90 cm in diameter. CF_4 is a high density gas which does not contain free protons. Thus the otherwise overwhelming inverse β-decay $\overline{\nu}_e p \to e^+ n$ does not occur. The TPC is surrounded by an anticompton shield (NE235 based liquid scintillator, attenuation length of 8 m at 430 nm), 50 cm thick, to convert and veto γ-rays which scatter in the gas and generate low energy recoil electrons. The scintillation light is detected by 48 EMI 8" photomultipliers, 24 on each

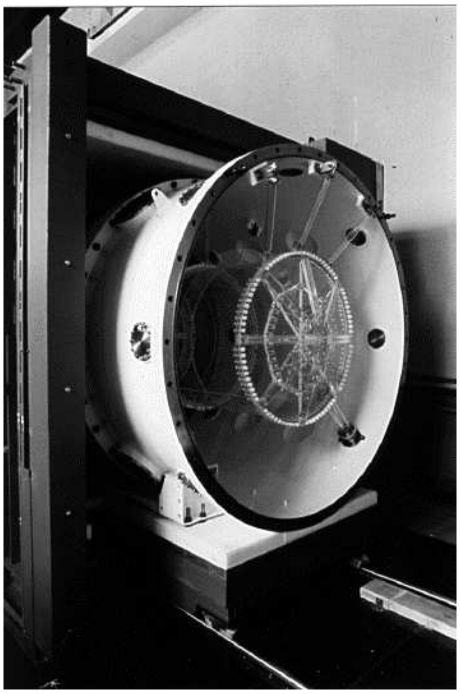

Figure 3.1: View of the TPC suspended in the scintillator tank.

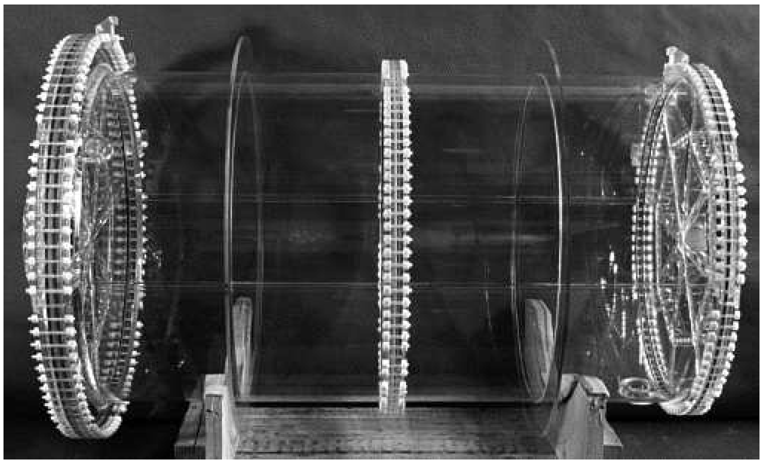

Figure 3.2: The acrylic vessel of the TPC.

lid. The liquid scintillator tank is shielded by 15 cm of lead. Neutrons generated by muon capture in the lead are attenuated and absorbed by 8 cm thick CH_2 plates covered with B_4C sheets. Details on the apparatus can be found in ref. [4].

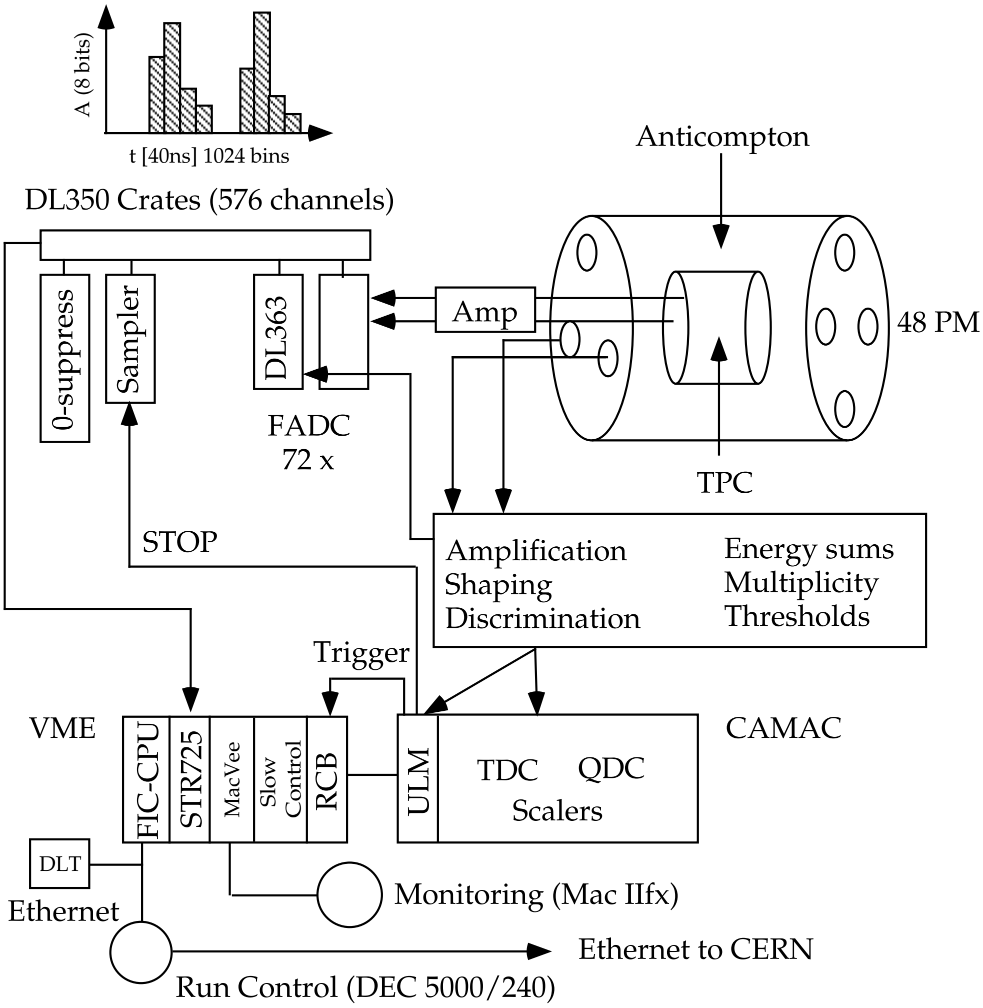

Figure 3.3: Electronics FADC readout and data acquisition system set up by the Zürich group. The photomultiplier readout was developed in collaboration with Grenoble.

Figure 3.1 shows a view of the TPC suspended in the liquid scintillator vessel. The TPC gas is enclosed in an acrylic container (Fig. 3.2). A field of 80 kV is applied between the cathode on one end of the container and the grid plane on the other end. Field shaping rings wrapped on the external circumference of the acrylic vessel provide a uniform electric field.

The z coordinate along the detector axis is calculated from the drift time. The drift velocity is 4 cm/μs at 120 V cm^{-1} bar^{-1}. Anode wires are electrically connected and provide the total energy of the electron and the timing signal for the TPC. Signals induced on the xy plane provide the two transverse coordinates. The xy plane is made of mylar covered on both sides by orthogonal copper strips with a pitch of 3.5 mm. There are 256 x and 256 y strips.

The 512 channels of x and y strips are preamplified and read out by flash ADC's (Struck DL350 system, see Fig. 3.3). We are thus able to visualize the electron track in three dimensions. The FADC response can be chosen non-linear to provide a uniform resolution even for small pulses. The pulses are sampled with 8 bits every 40 ns and stored in memories, 1024 locations deep, which thus cover the maximum drift time (40 μs) of the TPC. The data acquisition system is based on a FIC 8234 CPU running under the OS9 operating system.

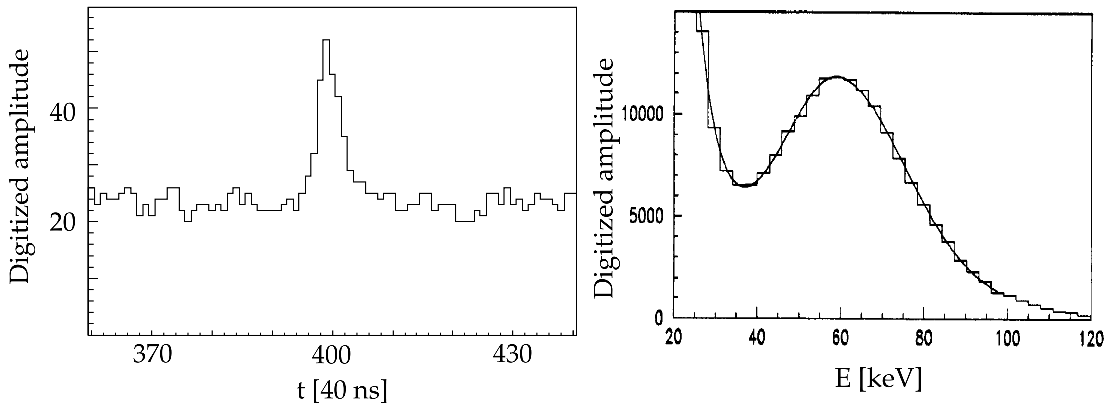

Figure 3.4: Left: amplitude distribution sampled by FADC from one photomultiplier for Čerenkov light induced by a passing muon. The signal is observed in coincidence with other photomutipliers. Right: measured energy distribution at 5 bar from the anode with 60 keV γ rays.

The Zürich group is responsible for the TPC readout and for the data acquisition system (Fig. 3.3) which is now fully implemented in the experimental area. Since several triggers (cosmic rays, neutrinos, radioactive sources, etc.) will be used, we are also preparing a general purpose trigger module (based on the LRS 2366 Universal Logic Unit, ULM) which will allow to adjust remotely the coincidences and timing for every trigger.

The FADC system is also used to read out the photomulipliers. The signals in the anti-compton shield generate on average less than one photoelectron in each of the photomultipliers for a veto threshold of 100 keV. The signals from several photomultipliers are therefore summed and shaped to a width of about 200 ns, larger than the sampling width (40 ns) of the FADC. Figure 3.4 shows the amplitude distribution from one photomultiplier from Čerenkov radiation induced by a cosmic muon traversing the acrylic vessel and detected in coincidence by at least 4 photomultipliers.

The full scale TPC has been operated in Neuchâtel at 3 bar with the FADC readout system using cosmic ray muons. Signals of the order of 10 mV were observed at 3 bar with an rms noise of less than 2 mV. The energy resolution was measured with 60 keV photons from an ^{241}Am source. Figure 3.4 shows the energy distribution of the anode signals. The resolution is $\sigma = 25$ % at 60 keV. Assuming that the resolution scales as the square root of the energy, we expect an energy resolution of $\sigma \simeq 10$ % at 500 keV.

A spatial resolution of $\sigma = 1.6$ mm has been achieved for the cathode strips by fitting muon tracks with straight lines. The mean attenuation length of drifting electrons at 3 bar was measured to be 22 $^{+14}_{-6}$ m [4]. Figure 3.5 shows the projections $x - z$ and $y - z$ of an electron track initiated by a photon from a radioactive source.

With a small prototype of the TPC and a ^{112}Sn radioactive source we measured the angular resolution of electrons [5]. We obtained an angular resolution of $\sigma_{\theta_{space}} = 13°$ for 370 keV electrons, in agreement with simulation.

The detector is now fully installed under the reactor. Electric noise problems in the readout chain of the TPC are being investigated before we proceed with final calibration and data taking.

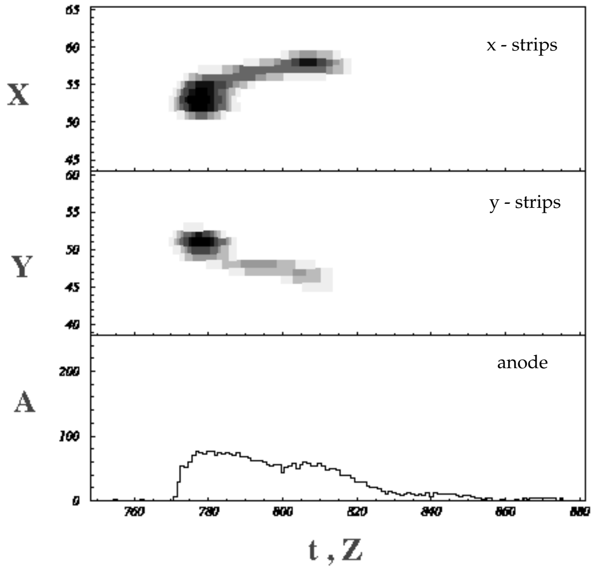

Figure 3.5: $x - z$ and $y - z$ views of a photon induced electron track, and time distribution of the anode pulse. Notice the larger ionization loss of the electron at the end of its trajectory (dark regions).

References

[1] E. K. Akhmedov *et al.*, Phys. Lett. **B 348** (1995) 124.

[2] F. Reines, H .S. Gurr and H.W. Sobel, Phys. Rev. Lett. **37** (1976) 315.

[3] P. Vogel and J. Engel, Phys. Rev. **D 39** (1989) 3378.

[4] C. Amsler *et al.*, Nucl. Instrum. Methods **A 396** (1997) 115.

[5] S. Iseli, diploma thesis, University of Zürich (1996).